PNAS
www.pnas.org

Supplementary Information for

Gastrointestinal dysfunction in autism displayed by altered motility and achalasia in *Foxp1*$^{+/-}$ mice

Henning Fröhlich, Marie Luise Kollmeyer, Valerie Catherine Linz, Manuel Stuhlinger, Dieter Groneberg, Amelie Reigl, Eugen Zizer, Andreas Friebe, Beate Niesler, and Gudrun Rappold

Correspondence to:
Prof. G.A. Rappold
gudrun.rappold@med.uni-heidelberg.de
phone: 49-6221-565059
fax: 49-6221-565155

This PDF file includes:

Other supplementary materials for this manuscript include the following:

www.pnas.org/cgi/doi/10.1073/pnas.1911429116

Supplementary Materials and Methods

Animals

Floxed *Foxp1* mice (1), Nestin-Cre deleter mice (2) and *Foxp1*$^{+/-}$ mice (3) were backcrossed with C57BL/6J mice for at least 12 generations to obtain congenic animals.

Animal studies were approved by the Regierungspräsidium Karlsruhe, Germany (approval nos. 35-9185.81/G-105/16 and 35-9185.81/G-86/14).

cDNA synthesis

Total RNA was prepared from frozen mouse GI tissue samples using peqGOLD TriFast™ (PEQLAB-Life Science). First strand cDNA synthesis was performed from 1.5 µg total RNA using a Superscript II reverse transcriptase kit (ThermoFisher Scientific, Waltham, MA, USA) and oligo dT_{12-18}-primers (ThermoFisher Scientific) according to the manufacturer's instructions.

Quantitative real-time PCR

Quantitative real-time PCR was performed using the qTOWER system (Analytic Jena, Jena, Germany) with an annealing temperature of 60°C using SYBR Green No-ROX Fast Mix (Bioline, Luckenwalde, Germany) according to the manufacturer's instructions. Each of the samples was analysed in triplicate and relative mRNA levels were assessed using the Standard Curve Method by normalization to succinate dehydrogenase complex subunit A (*Sdha1*) and hypoxanthine phosphoribosyltransferase 1 (*Hprt1*). All primer sequences are listed in Table S1.

Protein analysis

Protein isolation was performed using standard protocols. Western blot analysis was executed using the Odyssey Infrared Imaging System (LI-COR Biosciences, Lincoln, NE, USA). We used the following primary antibodies: rabbit anti-Foxp1 (Abcam, Cambridge, UK, Cat no. ab16645), rabbit anti-Nexilin (Abcam, Cambridge, UK, Cat no. ab233267), rabbit anti-Rbms3 (Thermo Fisher Scientific, Waltham, USA, Cat no. PA5-57028), rabbit anti-Gpr177/WLS (BIOZOL, Eching, Germany, Cat no. LS-B9704-100) and rabbit anti-GAPDH (Abcam, Cambridge, UK, Cat no. ab9485). IRDye 800CW goat anti-rabbit (LI-COR Biosciences, Lincoln, NE, USA) was used as a secondary antibody according to the manufacturer's instructions. Protein bands were quantified using Image Studio Lite 3.1 software (LI-COR Biosciences, Bad Homburg, Germany).

Tissue preparation for paraffin sections

Gastrointestinal tissue of mice at the age of P12.5 was fixed overnight in 4 % PFA/PBS, adult tissue by cardia perfusion following incubation in the fixative for three additional hours. Thereafter the tissue was dehydrated via an ethanol series and isopropanol. The tissue was cleared in toluene prior to infiltration and embedded in paraffin for sectioning.

Histological staining

Staining by hematoxylin and eosin stain as well as Masson-Goldner-Trichrome (Carl Roth, Karlsruhe, Germany) was performed on 3µm paraffin sections according to the manufacturer's instructions. After staining, the sections were dehydrated and embedded with DPX mountant (Sigma, Taufkirchen, Germany) and examined for histological changes by light microscopy.

Analysis of muscle thickness in the esophagus and colon

A minimum of six sections from at least 10 wildtype and 10 *Foxp1*$^{+/-}$ animals were analysed by a single observer in a blinded manner for two developmental stages (P12.5 and adult).

Immunofluorescence analysis

Immunostaining was performed on 10 µm paraffin sections using standard protocols. Sections were deparaffinized and rehydrated through an ethanol series; thereafter slides were incubated in citrate buffer for antigen retrieval. Cross sections of GI tissue were incubated overnight with primary antibodies at 4°C and incubated with appropriate fluorescent secondary antibodies for 1h at room temperature. The following primary antibodies were used: rabbit anti-Foxp1 (Abcam, Cambridge, UK, Cat no. ab16645) 1:100, rabbit anti-Ki67 (Abcam, Cambridge, UK, Cat no. ab16667) 1:100. Secondary antibody was Alexa Fluor 488 donkey anti-rabbit (ThermoFisher Scientific, Waltham, MA, USA, Cat no. A32790) (1:1000); DAPI (ThermoFisher Scientific) 1:1000 was used for nuclear staining.

TUNEL staining

Apoptotic cells were marked on 3µm paraffin sections using the *In Situ* Cell Death Detection Kit, Fluorescein (Roche, Penzberg, Germany) according to the manufacturer's instructions.

Microscopy

At the Nikon Imaging Center (University of Heidelberg), the Nikon Ni-E research microscope was used for brightfield and widefield microscopy. The images were taken by the software NIS-Elements acquisition (version 4.5). The fluorescent samples were imaged with the Nikon DS-Qi1Mc black and white camera. Histological sections were imaged with a brightfield Nikon DS-Ri1 colour camera.

Image processing was based on the "ethical guidelines for the appropriated use and manipulation of scientific digital images" (4) and was performed with ImageJ and Adobe Photoshop.

Isometric force studies

Animals were killed by cervical dislocation. The abdomen was opened and the entire gastrointestinal tract quickly removed and transferred to Krebs-Henseleit solution (118 mM NaCl, 4.7 mM, KCl, 2.5 mM $CaCl_2$, 1.2 mM KH_2PO_4, 1.2 mM $MgSO_4$, 25 mM $NaHCO_3$, pH 7.4, 7.5 mM glucose) bubbled with 95% O_2 / 5% CO_2. Lower esophagus sphincter (LES), pylorus and fundus strips were isolated and mounted on fixed

segment support pins in the organ bath (Myograph 610; Danish Myo Technology, Aarhus, Denmark) containing 5 ml of Krebs-Henseleit solution. The resting tension was set to 3 mN and rings/strips were pre-contracted with carbachol (CCh; 1 µM) (Sigma, Taufkirchen, Germany). Relaxation was induced with DEA-NO (Axxora, Lörrach, Germany) as indicated. At the end of each experiment, isobutylmethylxanthine (IBMX) (Sigma, Taufkirchen, Germany) was added to induce maximal relaxation (defined as 0 % contraction).

Total gut transit

Carmine (50 µl; 3 mg carmine in 0.5% methylcellulose) (Sigma, Taufkirchen, Germany) was orally administered to each mouse. Mice were then returned to individual cages and placed on a white sheet of paper. The time until excretion of the first coloured faeces was recorded.

Whole colon preparation

The animals were killed by cervical dislocation. The abdomen was opened and the whole intestine was quickly removed and transferred to 4 °C cold Krebs-Henseleit solution bubbled with 95% O_2 / 5% CO_2. The mesentery was completely removed and faecal content was gently flushed out. To enable perfusion of the colon, small tubes were fixed at the proximal and distal part of the colon. The isolated colon was then mounted in a chamber filled with 300 ml Krebs-Henseleit buffer which was kept at 37 °C and bubbled with 95% O_2 / 5% CO_2. Within 60 min, spontaneous contractions developed which started in the proximal part and propagated distally along the whole colon. Videos were subsequently recorded for 30 min using a webcam (Logitech® HD Webcam C525). During the experiment, the colon was perfused with PBS (flowrate 30 µl min^{-1}).

Video recordings were transferred into spatiotemporal maps using a Plugin (gMapsON) for ImageJ written by S.P. Parsons (http://www.scepticalphysiologist.com/code/code.html).

Esophageal manometry

The mice were anaesthetized with pentobarbital (50 mg kg–1 I.P.). Esophageal manometry was performed using a customized catheter (Dentsleeve International, Ltd, Ontario, Canada; perfusion pressure 10 kilopascal (kPa) connected to a perfusion pump (Mui-Scientific, Ontario, Canada) via pressure transducers (Alpine Biomed GmbH, Langenfeld, Germany) and 0.01 ml resistor catheters (Dentsleeve International, Ltd., Mississauga, ON, Canada). The transducers were connected to a Polygraf-ID recorder (Medtronic GmbH, Meerbusch, Germany), and pressure data were evaluated using the Polygraf NET-software (Medtronic Polygram Net, version 4.2.95.80; Medtronic). The catheter was introduced antegrade and fixed with the very distal opening in the lower esophageal sphincter (LES) area. Swallows were induced by a mechanical irritation and activity was monitored for 30 min.

Affymetrix mRNA microarray

Striata were dissected from the brains of E18.5 and P1.5 WT and Nestin-Cre/*Foxp1*$^{-/-}$ mice in ice-cold PBS. RNA was prepared using Trizol, according to the manufacturer's instructions. Gene expression profiling was performed using GeneChip® Mouse Gene 2.0 ST Arrays from Affymetrix (Santa Clara, CA, US). cDNA and cRNA synthesis and hybridization to arrays were performed according to the recommendations of the manufacturer. A Custom CDF Version 17 with Entrez based gene definitions was used to annotate the arrays. The Raw fluorescence intensity values were normalized applying quantile normalization. Differential gene expression was analysed with OneWay-ANOVA using a commercial software package SAS JMP10 Genomics, version 6, from SAS (SAS Institute, Cary, NC, US). A false positive rate of a=0.05 with FDR correction was taken as the level of significance. Gene Set Enrichment Analysis (GSEA) was used to determine whether defined sets of genes exhibit a statistically significant bias in their distribution within a ranked gene list (see http://www.broadinstitute.org/gsea). Pathways belonging to various cell functions were obtained from public external databases (KEGG, http://www.genome.jp/kegg/) and biological functions from the Gene Ontology analysis (GOBP, http://www.geneontology.org/).

Statistics

IBM SPSS STATISTICS 21 and Microsoft Excel were used to analyse the data. Outliers were determined via IBM SPSS STATISTICS 21 and extreme outliers (≥ 3 standard deviations above mean) excluded from further analysis. All data were checked for normal distribution via the Kolmogorov-Smirnov and Shapiro-Wilk test. If appropriate, one-way ANOVA was performed, in which litter was used as covariate (ANCOVA). In all other cases, unpaired two-tailed Student's t-tests served to compare differences between the two groups. *P* values of ≤ 0.05 were considered significant.

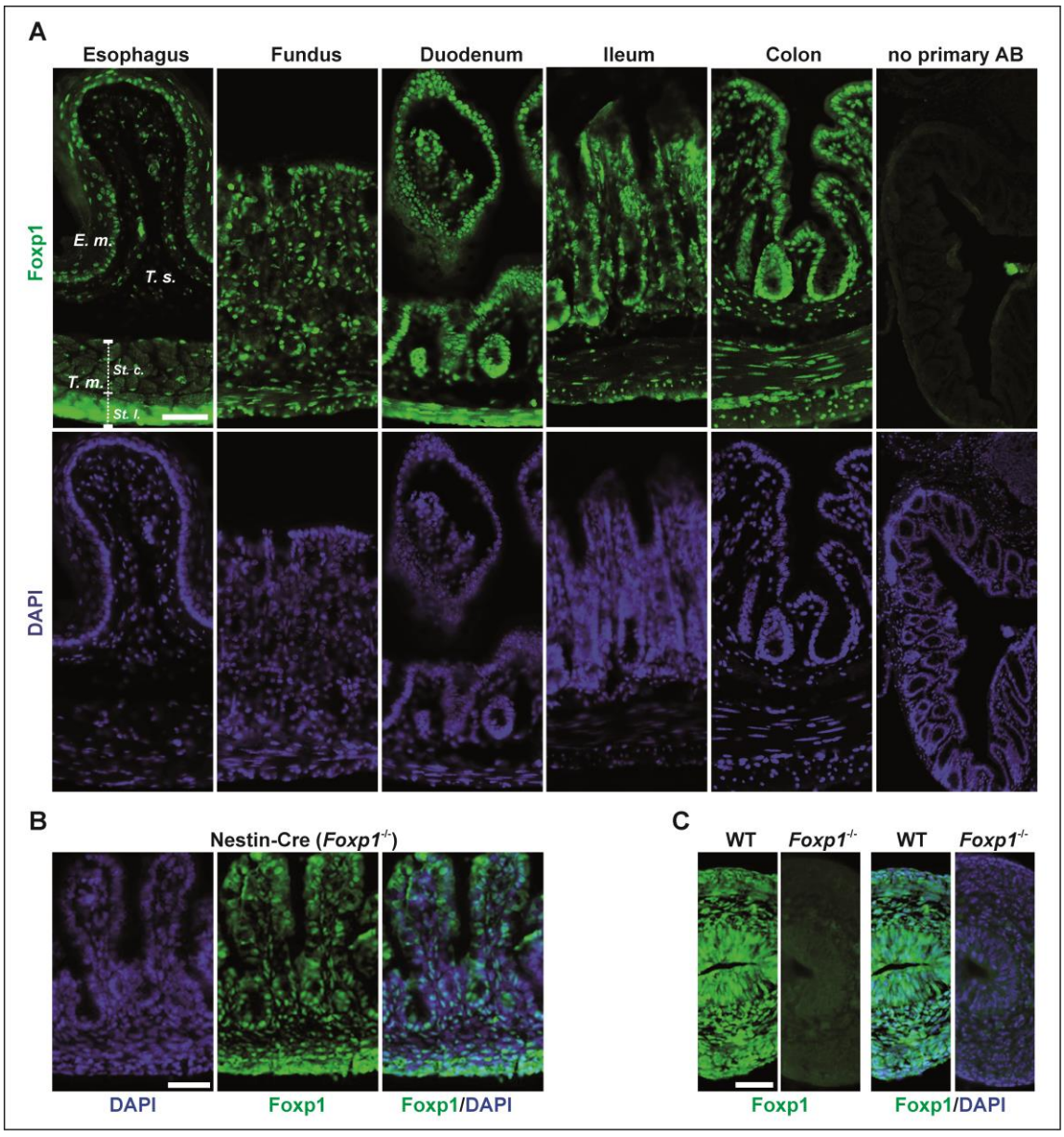

Fig. S1. **Foxp1 expression in different regions of the murine gastrointestinal tract. A**, Foxp1 expression by immunofluorescence staining is indicated in green and shows ubiquitous expression in the esophagus, fundus, duodenum, ileum, and colon of adult animals (10 weeks old). Nuclei (blue) were counter-stained with DAPI. Foxp1 is ubiquitously expressed in nuclei of various cell types residing within all layers of the gut wall. **B**, At E18.5 the Nestin-Cre (*Foxp1*$^{-/-}$) midgut reveals normal Foxp1 expression (apart from enteric neurons which are not shown in this picture). **C,** Foxp1 antibody specificity was confirmed by staining sections of WT and *Foxp1*$^{-/-}$ midgut at E13.5. Tunica mucosa (T. m.), stratum circulare (St. c.), stratum longitudinale (St. l.), tela submucosa (T. s.), epithelium mucosae (E. m.); scale bar corresponds to 50 µm.

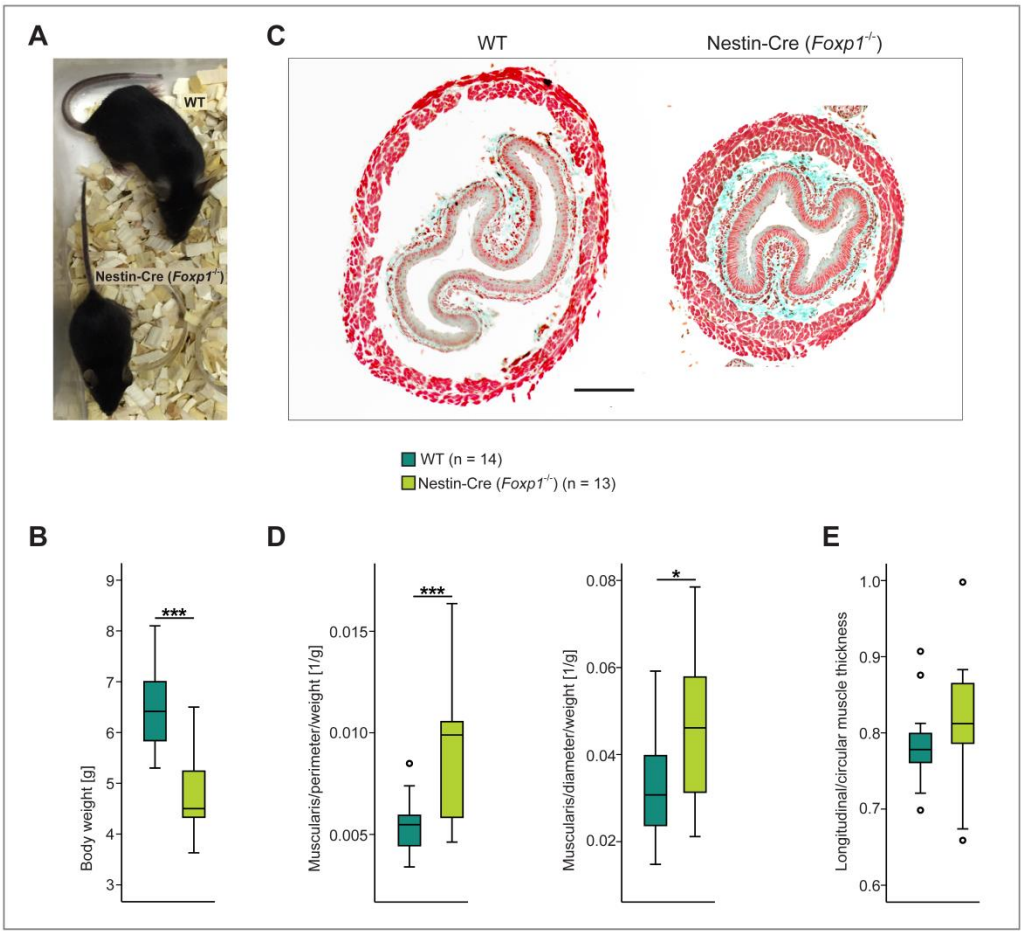

Fig S2. **Nestin-Cre (*Foxp1*$^{-/-}$) mice display thriving difficulties and increased thickness of the esophageal muscle layer. A**, Nestin-Cre (*Foxp1*$^{-/-}$) mice exhibit a pronounced reduction in size compared to WT animals at adult stage. **B**, Body weight is already strongly reduced in Nestin-Cre (*Foxp1*$^{-/-}$) animals by 26% at P12.5. **C**, cross sections of a WT and Nestin-Cre (*Foxp1*$^{-/-}$) esophagus at P12.5. **D**, the tunica muscularis shows an increased thickness in Nestin-Cre (*Foxp1*$^{-/-}$) mice at P12.5. Muscle thickness was normalized against perimeter and diameter together with body weight. **E**, the ratio of longitudinal to circular muscle thickness does not differ between WT and Nestin-Cre (*Foxp1*$^{-/-}$) tissue at P12.5, indicating that both layers are equally affected in Nestin-Cre (*Foxp1*$^{-/-}$) mice. Sections were stained with Masson-Goldner-Trichrome. For the box-and-whisker plot, the boxes represent the first and third quartiles, the whiskers are 95% confidence interval, and the lines within the boxes are median values. Weak outliers are marked with a circle. Black asterisks indicate significant difference (**P* ≤0.05, ***P* ≤ 0.01, ****P* ≤ 0.001, unpaired two-tailed Student's t-test); scale bar corresponds to 100 µm.

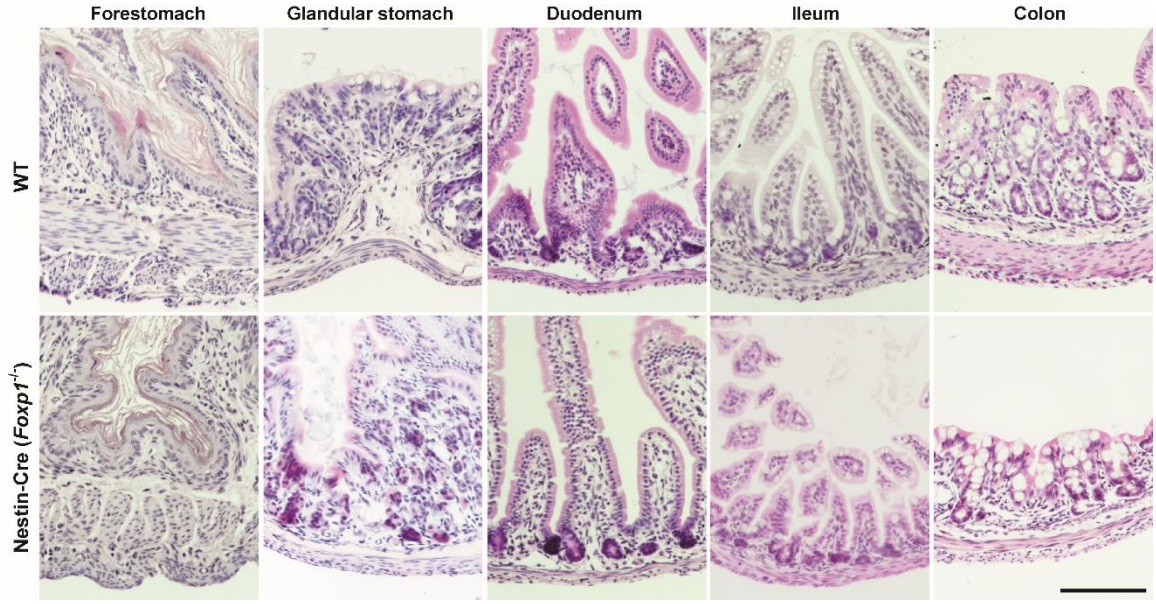

Fig. S3. **Nestin-Cre (*Foxp1*$^{-/-}$) mice do not show obvious morphological alterations in the stomach, duodenum, ileum and colon at P12.5.** Tissue sections were stained with hematoxylin and eosin, n = 3 WT/3 Nestin-Cre (*Foxp1*$^{-/-}$) animals were evaluated; scale bar corresponds to 100 µm.

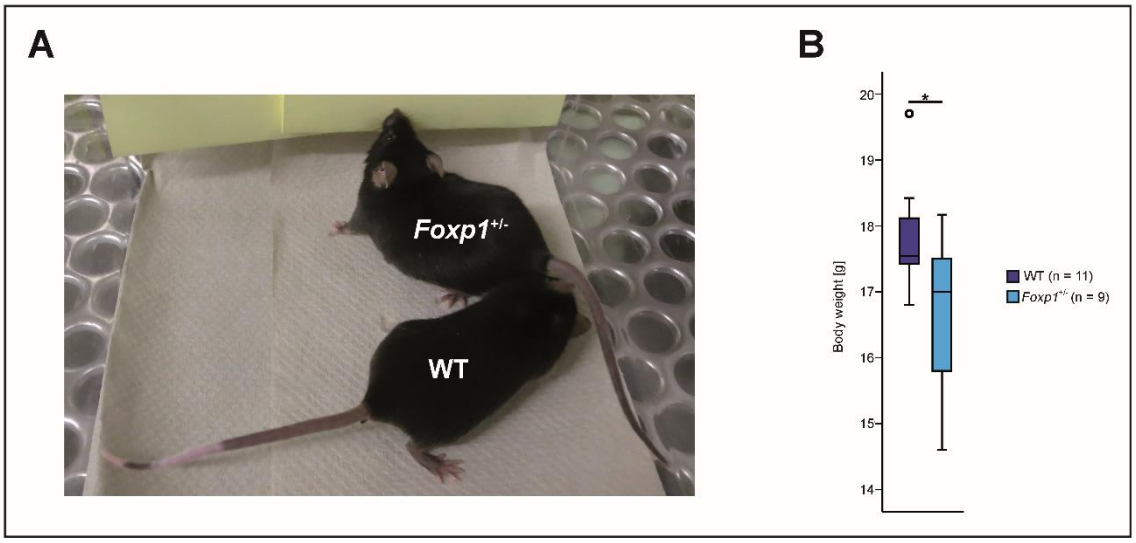

Fig. S4. **Adult *Foxp1*$^{+/-}$ mice do not show obvious differences in body size compared to WT littermates although their body weight is reduced. A**, male WT and *Foxp1*$^{+/-}$ mouse in comparison. **B**, also female *Foxp1*$^{+/-}$ mice show a significant reduction in body weight compared to WT animals at the age of eight weeks.

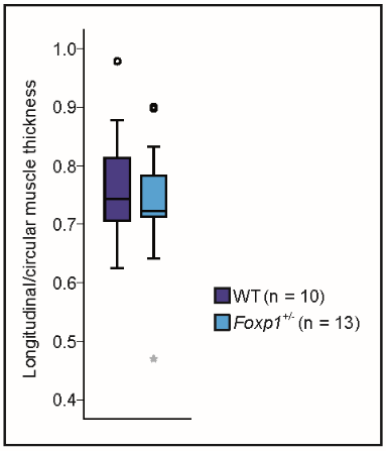

Fig. S5. **Both layers of the tunica muscularis are equally affected in the *Foxp1*$^{+/-}$ esophagus at P12.5.** The thickness of circular and longitudinal muscle layer was determined on cross sections of WT and *Foxp1*$^{+/-}$ esophagus. The ratio of longitudinal to circular muscle thickness did not differ between WT and *Foxp1*$^{+/-}$ tissue indicating that both layers are equally affected in *Foxp1*$^{+/-}$ mice. For the box-and-whisker plot, the boxes represent the first and third quartiles, the whiskers are 95% confidence interval, and the lines within the boxes are median values. Weak outliers are marked with a circle; strong outliers marked with a small grey asterisk were excluded from statistical calculation (ANCOVA).

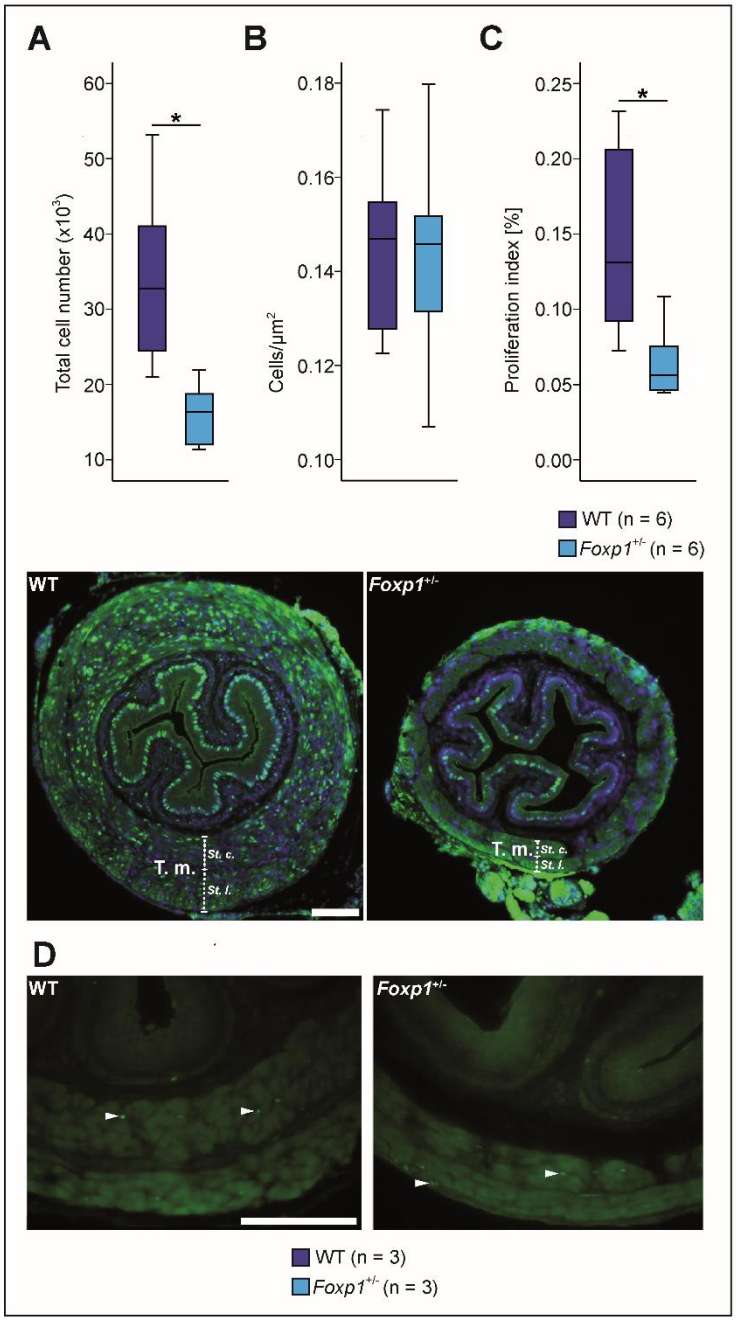

Fig. S6. **Reduced cell number and proliferation rate in the tunica muscularis of the *Foxp1*$^{+/-}$ esophagus.** Ki67 staining (green) in WT and *Foxp1*$^{+/-}$ cross sections at P12.5; nuclei (blue) were stained by DAPI. **A**, the tunica muscularis in *Foxp1*$^{+/-}$ tissue shows 53 % less cells compared with WT tissue. **B**, the cell density within the tunica muscularis did not differ between WT and *Foxp1*$^{+/-}$ esophagus. **C**, *Foxp1*$^{+/-}$ animals exhibit a reduced proliferation index by 55 % in the tunica mucosa compared with WT mice with less Ki67-positive cells per cells in total. **D**, TUNEL staining (green) did not reveal apoptotic cells in the tunica muscularis, neither in WT nor in *Foxp1*$^{+/-}$ tissue. Arrowheads mark unspecific staining (autofluorescent erythrocytes). For the box-and-whisker plot, the boxes represent the first and third quartiles, the whiskers are 95% confidence interval, and the lines within the boxes are median values. Black asterisk indicates significant difference (*$P \leq 0.05$, ANCOVA). Tunica mucosa (T. m.), stratum circulare (St. c.), stratum longitudinale (St. l.); scale bar corresponds to 100 µm.

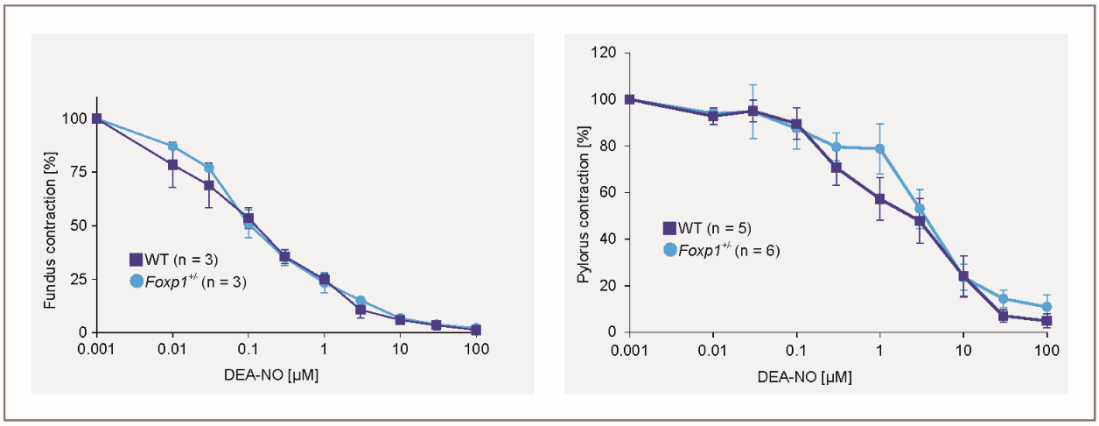

Fig. S7. **Contractility of fundus and pylorus in *Foxp1*$^{+/-}$ mice compared to WT animals.** Quantitative analysis of organ bath experiments from WT and *Foxp1*$^{+/-}$ mice showing DEA-NO-induced relaxation in fundus and pylorus after pre-contraction with 1 µM CCh. No significant differences were observed between *Foxp1*$^{+/-}$ and WT tissue. 2-(N,N-diethylamino)-diazenolate-2-oxide.diethylammonium salt (DEA-NO); carbachol (CCh).

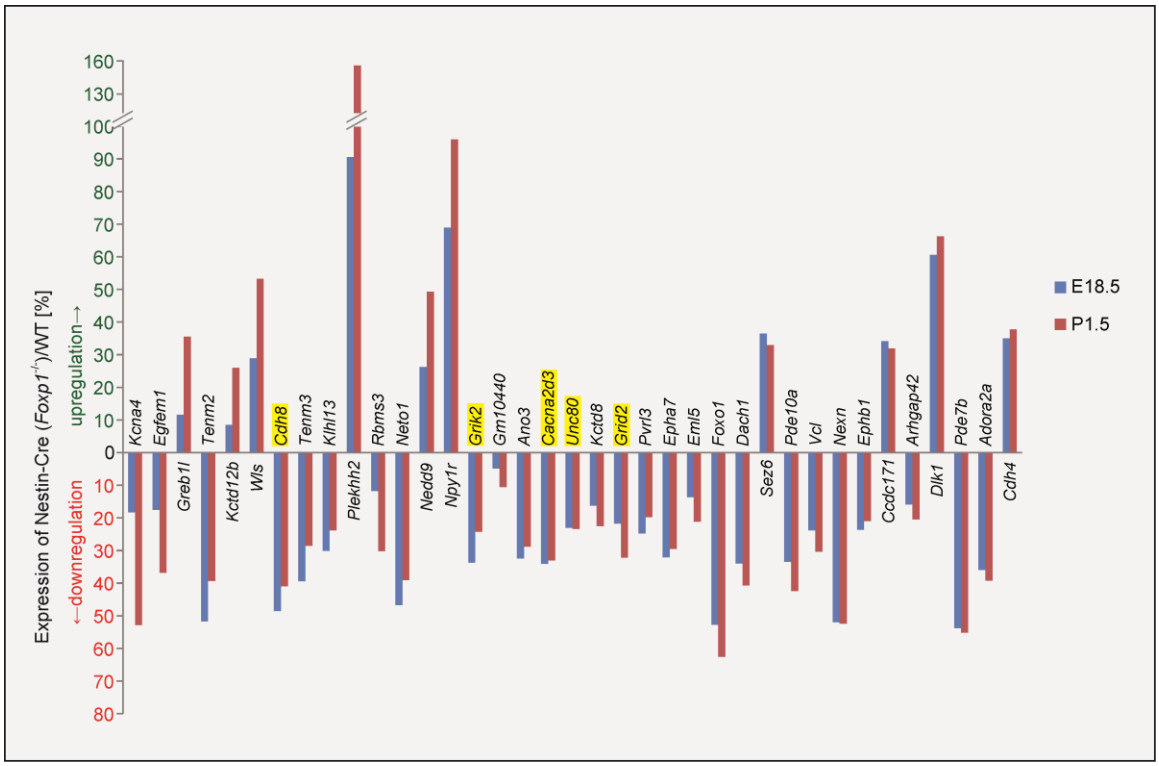

Fig. S8. **Genes with a significantly altered expression in striatal tissue from Nestin-Cre (*Foxp1*$^{-/-}$) animals compared to WT at two developmental stages, E18.5 and P1.5.** Microarray experiments were performed at E18.5 and P1.5. At both developmental stages, striatal tissue from six Nestin-Cre (*Foxp1*$^{-/-}$) and six WT animals was used. Thirty-seven genes exhibited an altered expression in Nestin-Cre (*Foxp1*$^{-/-}$) mice at both stages (27 genes were down- and 10 genes were significantly upregulated at both time points). Genes are sorted by expression difference between E18.5 and P1.5 (highest expression difference on the left side of the figure). Autism risk genes (*Cacna2d3*, *Cdh8*, *Grik2*, *Unc8* and *Grid2*) are highlighted in yellow.

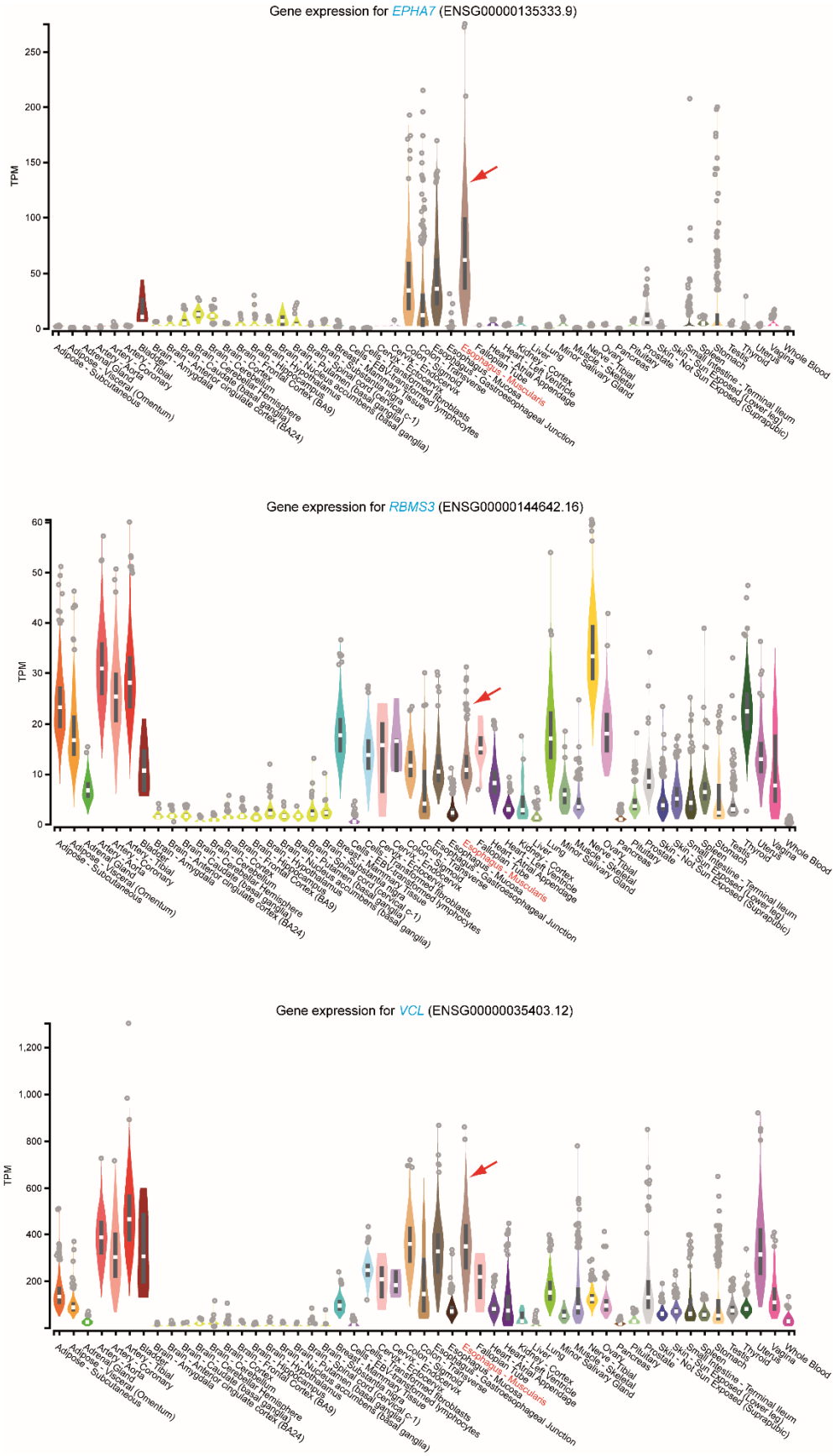
Gene expression for EPHA7 (ENSG00000135333.9)
Gene expression for RBMS3 (ENSG00000144642.16)
Gene expression for VCL (ENSG00000035403.12)
TPM
Esophagus - Mucosa
Esophagus - Muscularis

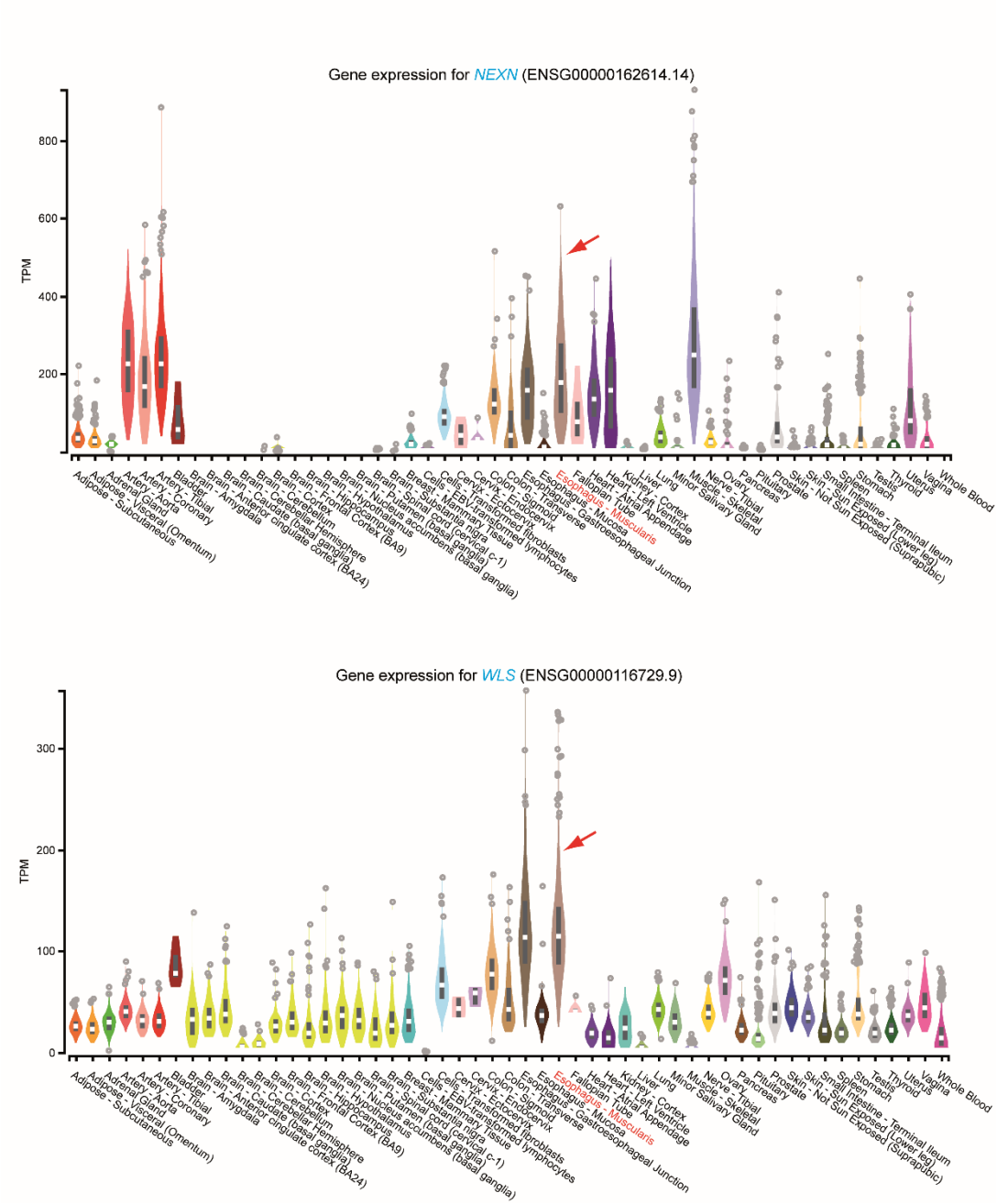

Fig. S9. ***Epha7, Nexn, Rbms3, Vcl* and *Wls* are highly expressed in the human esophagus.** RNA-Seq data from the GTEX portal was used to evaluate the esophageal expression of the 37 genes that were deregulated in the Nestin-Cre (*Foxp1*$^{-/-}$) striatum at E18.5 and P1.5. *Epha7*, *Nexn*, *Rbms3*, *Vcl* and *Wls* showed the strongest expression in esophageal tissue. TPM, transcripts per million.

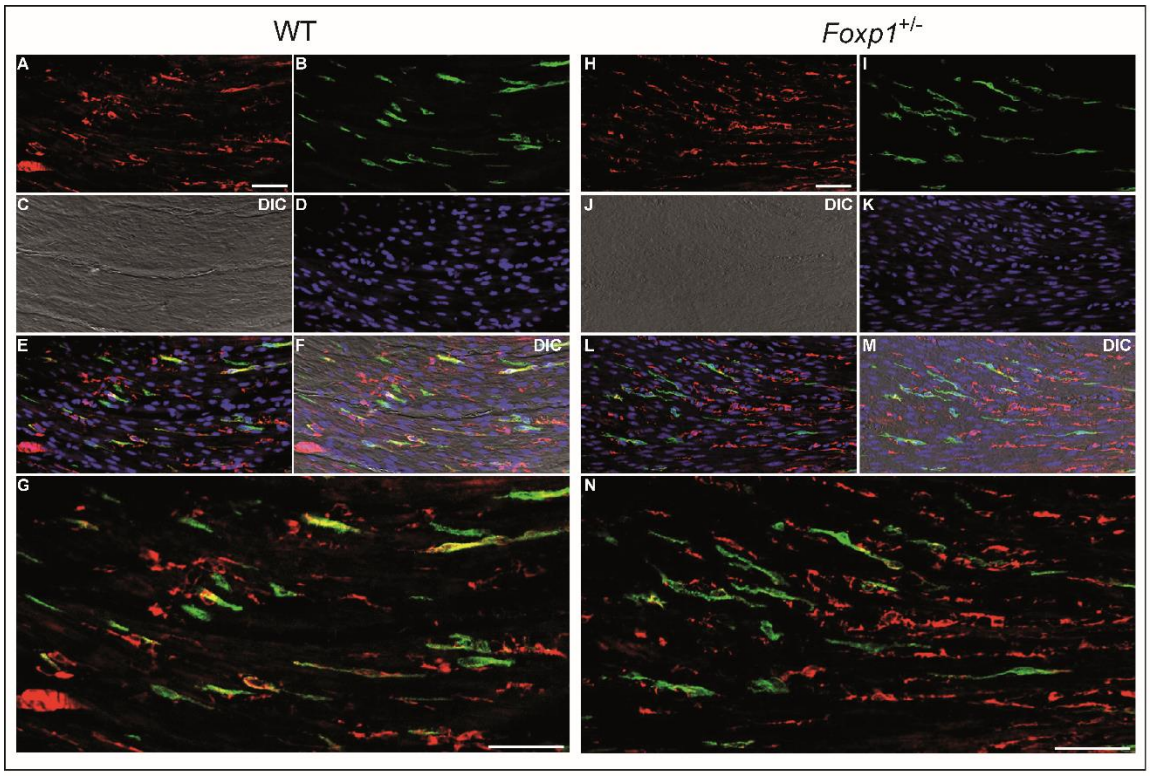

Fig. S10. **The number of interstitial cells of Cajal in the lower esophageal spincter does not differ between adult WT and *Foxp1*$^{+/-}$ mice.** Immunofluorescence staining of cKit (green) was used to mark the interstitial cells of Cajal (B, E, F, G, I, L, M, N). No difference in number was detected between WT and *Foxp1*$^{+/-}$ tissue. Also the NO-sensitive guanylyl cyclase (counter-stained in red) which modulates the lower esophageal spincter tone did not show expression differences between the two genotypes (A, H, E, F, G, L, M, N). Nuclei (blue) were stained with DAPI (D, K, E, F, L, M), scale bar corresponds to 50 µm, differential interference contrast (DIC), n = 3 WT/3 *Foxp1*$^{+/-}$.

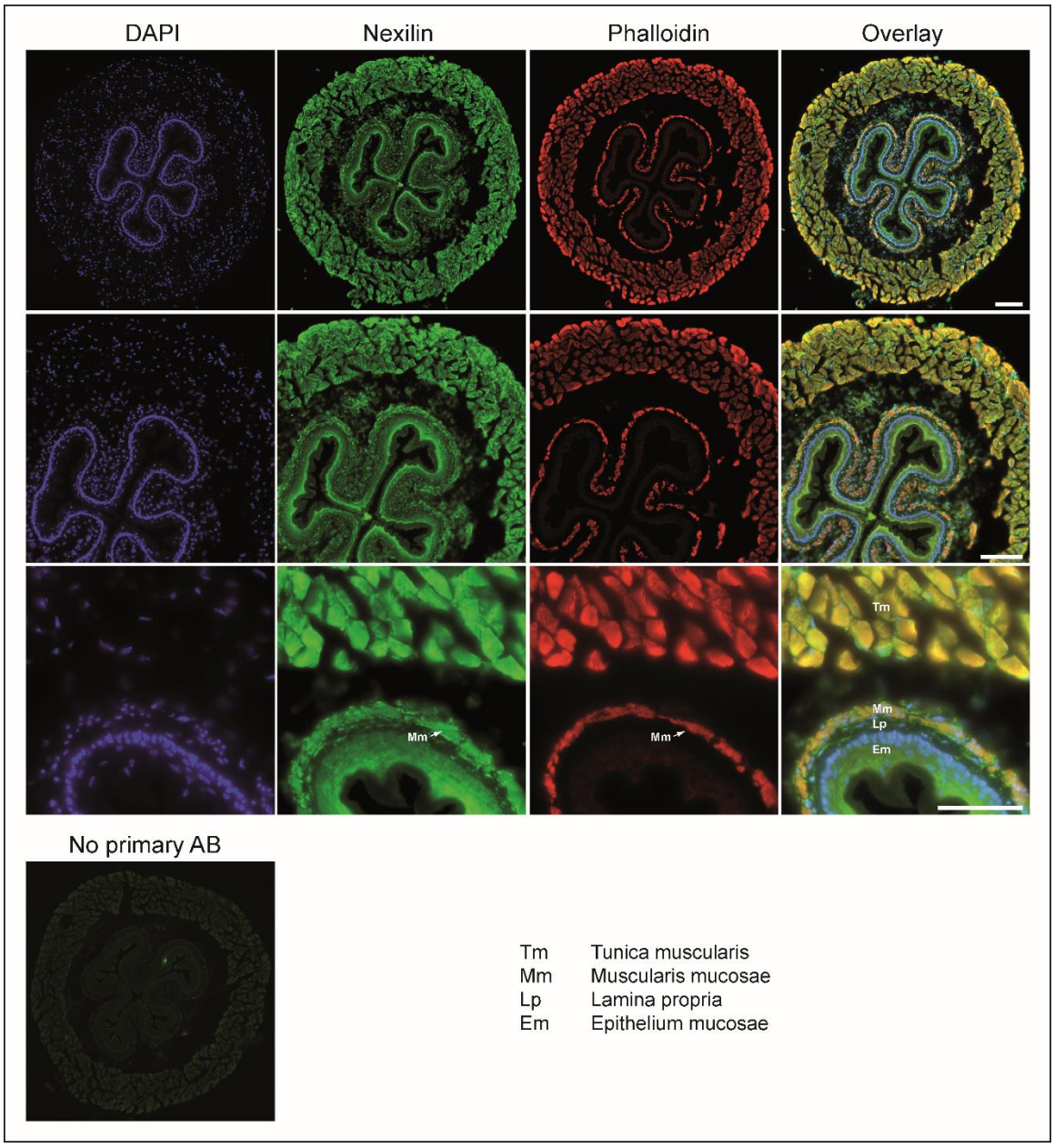

Fig. S11. **Expression of Nexn in the distal esophagus of the adult WT mouse.** Nexilin expression by immunofluorescence staining is indicated in green, Phalloidin-TRITC (red) was used to mark actin. As expected for an actin filament-binding protein, nexilin expression overlaps with the actin expression and is strongest in the tunica muscularis and muscularis mucosae. Scale bar corresponds to 100 µm.

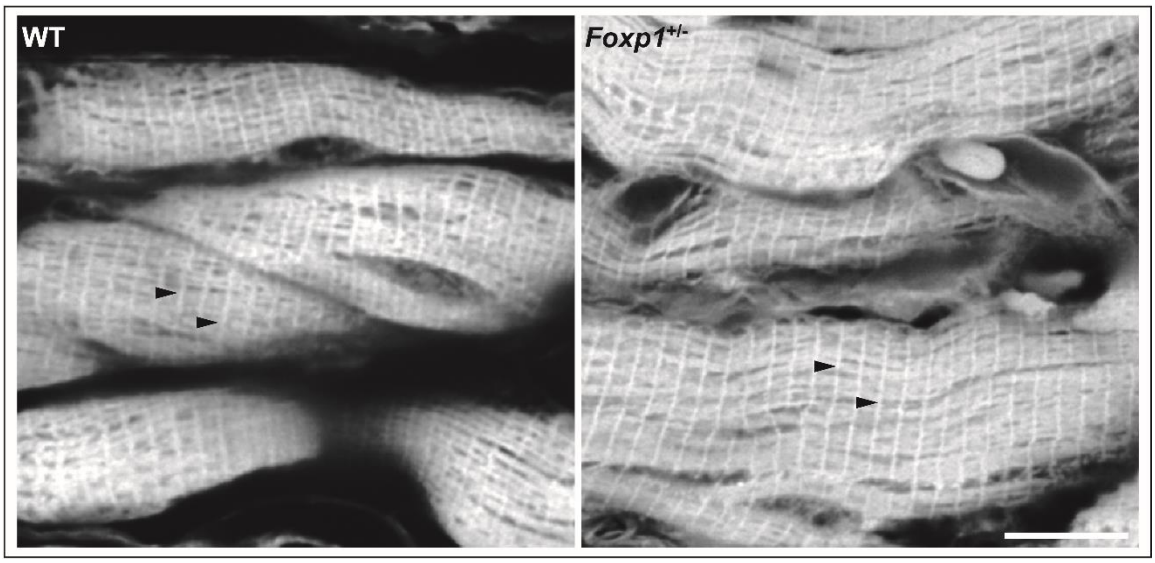

Fig. S12. **F-actin and sarcomer structure in the tunica muscularis do not show obvious alterations in the adult *Foxp1*$^{+/-}$esophagus.** Cross sections of the distal WT and *Foxp1*$^{+/-}$ esophagus were stained with phalloidin-TRITC to mark the F-actin. Sarcomer and F-actin structure were evaluated by confocal microscopy. Arrowheads indicate Z-disks, scale bar corresponds to 10 µm, n = 3 WT/3 *Foxp1*$^{+/-}$.

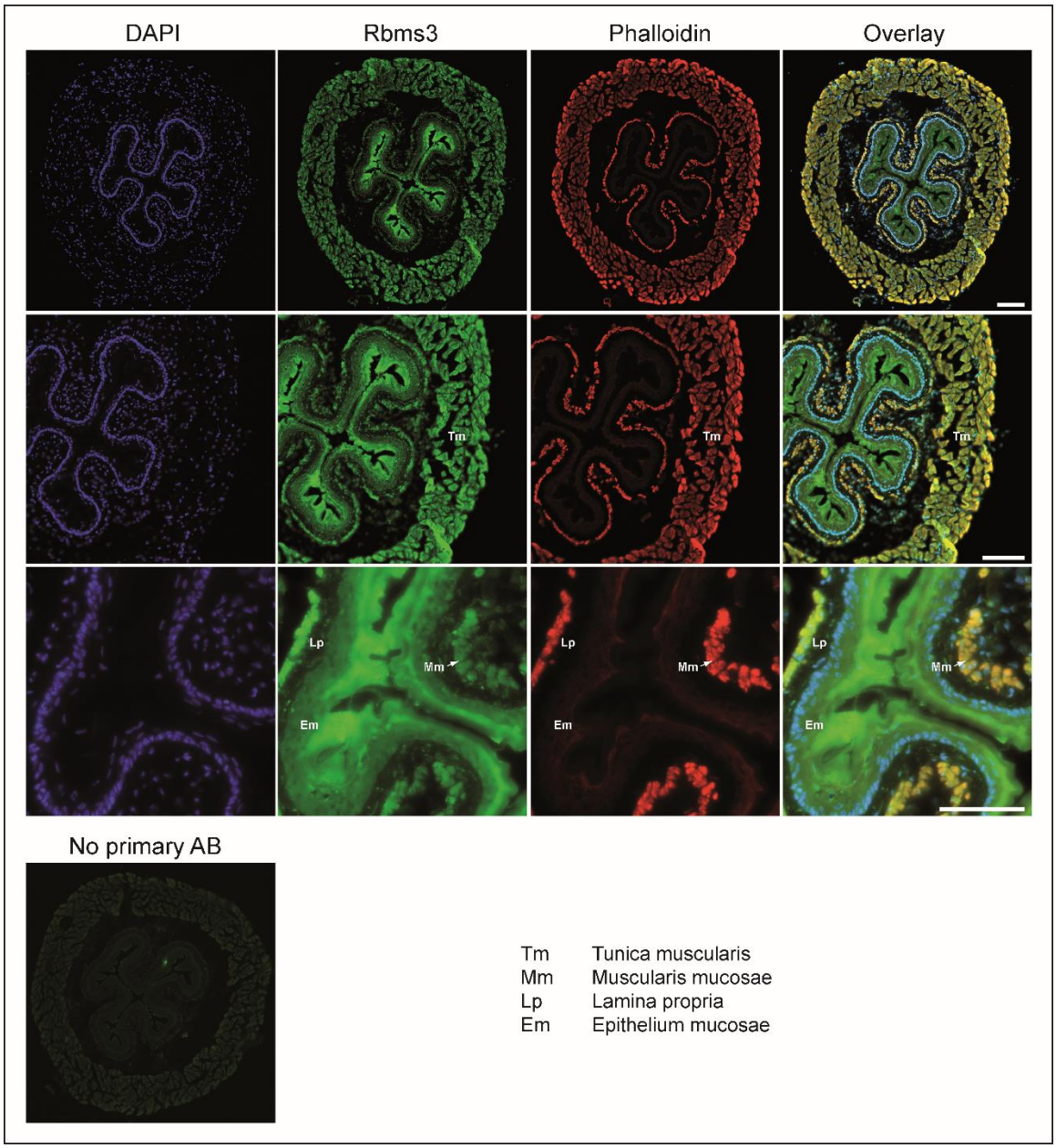

Fig. S13. **Expression of Rbms3 in the distal esophagus of the adult WT mouse.** RNA binding motif single stranded interacting protein 3 expression by immunofluorescence staining is indicated in green, Phalloidin-TRITC (red) was used to mark actin. Rbms3 shows a ubiquitous expression throughout the esophageal wall with a high expression in both smooth muscle (muscularis mucosae) and skeletal muscle (tunica muscularis) and the epithelium. Scale bar corresponds to 100 µm.

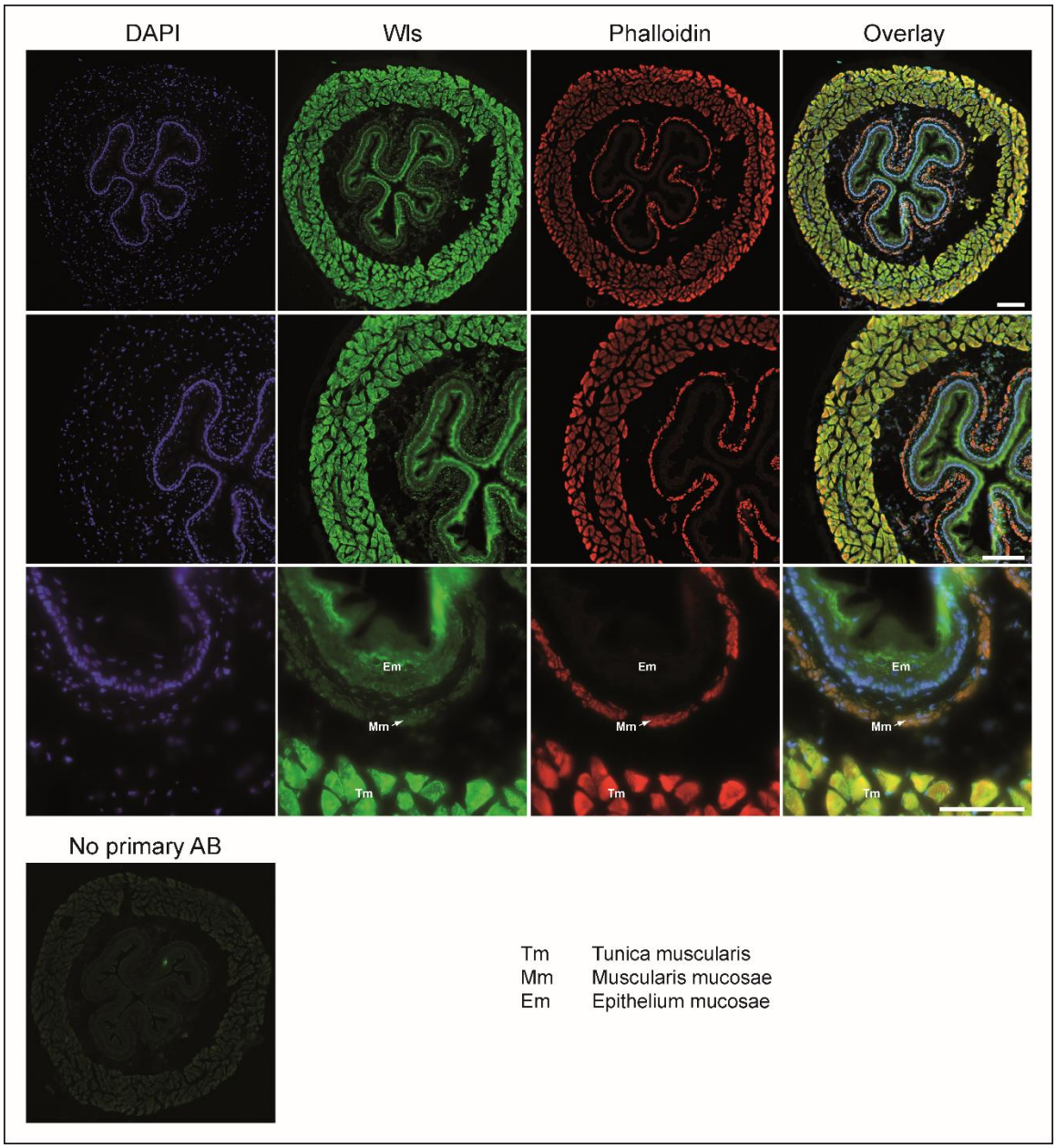

Fig. S14. **Expression of Wls in the distal esophagus of the adult WT mouse.** Wntless expression by immunofluorescence staining is indicated in green, Phalloidin-TRITC (red) was used to mark actin. Wntless is expressed throughout the esophageal wall but shows its highest expression in the tunica muscularis. Scale bar corresponds to 100 µm.

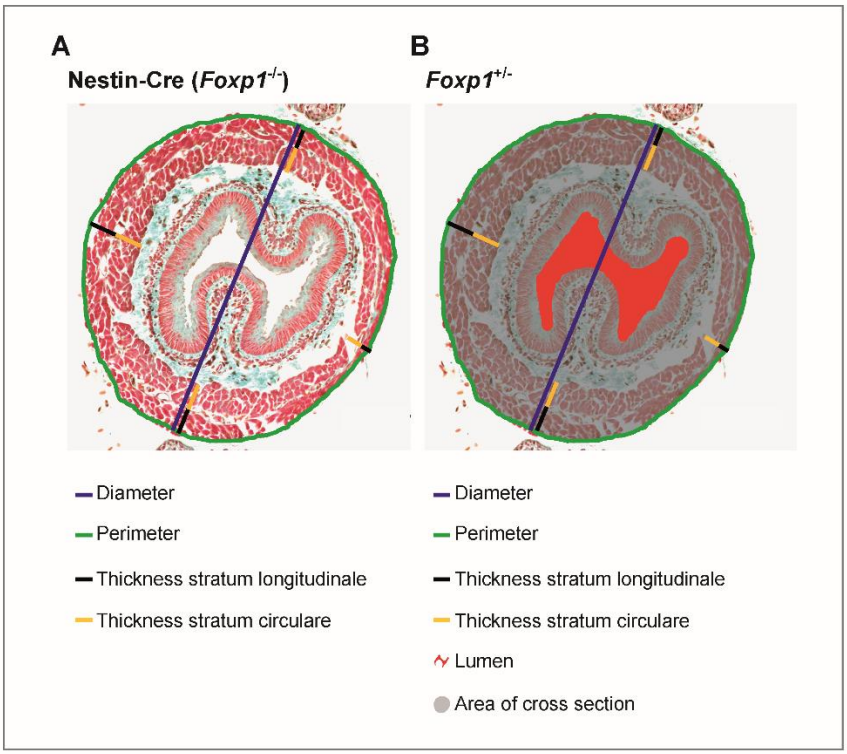

Fig. S15. **Methodology of the histological analysis in Nestin-Cre (*Foxp1*$^{-/-}$) and *Foxp1*$^{+/-}$ cross sections of the esophagus.** ImageJ software was used to determine changes in esophageal morphology between WT and Nestin-Cre (*Foxp1*$^{-/-}$) or *Foxp1*$^{+/-}$ tissue. **A**, histological analysis of Nestin-Cre (*Foxp1*$^{-/-}$) tissue. The thickness of the inner and outer muscular layer was taken at four opposite sides and perimeter and diameter were measured for each section. Nestin-Cre (*Foxp1*$^{-/-}$) mice are much smaller than WT animals, therefore all values were normalized to the body weight of the respective animal. **B**, histological analysis of *Foxp1*$^{+/-}$ tissue. In contrast to Nestin-Cre (*Foxp1*$^{-/-}$) mice, *Foxp1*$^{+/-}$ animals do not differ in size compared to WT animals and in young adult mice body weight is only slightly reduced. To include organ size in our calculations, we normalized all values to the area of the respective cross section.

Gene	Primer sequence 5' → 3'
Foxp1 for	GGCGGTGGGGGTTGTTGGAG
Foxp1 rev	AGAGCGCCTGCAAGCCATGA
Nexn for	AGGCGAGCAATTGACCTTGA
Nexn rev	ACCTGGCTTTCATGTTCACCT
Epha7 for	CCGGGAACAGTGTACGTCTT
Epha7 rev	CGAACACCATGAACACCAAG
Wls for	TAATGGTGACCTGGGTGTCC
Wls rev	TCCTGTGCTTCTTTACGGGTC
Vcl for	GATGAGGAGTCTGAGCAGGC
Vcl rev	AAAGCCAGCATCTGTTCGGA
Rbms3 for	CTGCTCCTATGCAAGGGACC
Rbms3 rev	ACCGTCTGGGGAGAGGTATC
Hprt1 for	TCCTCCTCAGACCGCTTTT
Hprt1 rev	CCTGGTTCATCATCGCTAATC
Sdha1 for	CATGCCAGGGAAGATTACAAA
Sdha1 rev	GTTCCCCAAACGGCTTCT
Foxp1 flox for	CTCCTAGTCACCTTCCCCAGTGC
Foxp1 flox rev	GAACACTGTCGAATGACCCTGC
Nestin-Cre for	AGTGCTGACTCTCCTCGGCTT
Nestin-Cre rev	CCAGACCTGTTCCACCTCTG
Foxp1 geno for	CCTCTGGCGATGAACCTAGTGGTTC
Foxp1 geno rev	AGCCACACTTTCTCTCAGGATGTCC
Foxp1 geno neo	AGCGCATGCTCCAGACTGCCTTG

Table S1. **Primers used in real-time PCR analysis and genotyping of animals are listed.**

Video S1 (separate file). Spontaneous colon contractions, WT.

Video S2 (separate file). Spontaneous colon contractions, *Foxp1*$^{+/-}$.

Dataset S1 (separate file). Microarray data showing significantly dysregulated genes in the striatum of Nestin-Cre (*Foxp1*$^{-/-}$) mice at E18.5 and P1.5. The 37 genes that are dysregulated at both developmental stages are marked in red.

References

1. Feng X, Ippolito GC, Tian L, Wiehagen K, Oh S, Sambandam A *et al.* Foxp1 is an essential transcriptional regulator for the generation of quiescent naive T cells during thymocyte development. *Blood* 2010; **115**(3)**:** 510-518.

2. Tronche F, Kellendonk C, Kretz O, Gass P, Anlag K, Orban PC *et al.* Disruption of the glucocorticoid receptor gene in the nervous system results in reduced anxiety. *Nat Genet* 1999; **23**(1)**:** 99-103.

3. Wang B, Weidenfeld J, Lu MM, Maika S, Kuziel WA, Morrisey EE *et al.* Foxp1 regulates cardiac outflow tract, endocardial cushion morphogenesis and myocyte proliferation and maturation. *Development* 2004; **131**(18)**:** 4477-4487.

4. Cromey DW. Avoiding twisted pixels: ethical guidelines for the appropriate use and manipulation of scientific digital images. *Sci Eng Ethics* 2010; **16**(4)**:** 639-667.